**RESEARCH ARTICLE**

# Incorporation of Nickel with Azo Dye and its Applications in Dye-Sensitized Solar Cells

Eman H. Sahap*, Fatima A. A. Sajad, Hutham M. Y. Al-Labban

*Faculty of Science, Department of Chemistry, University of Kufa, Kufa, Iraq*

***Received: 22nd February, 2022; Revised: 20th April, 2022; Accepted: 10th May, 2022; Available Online: 25th June, 2022***

**ABSTRACT**

Titanium dioxide ($TiO_2$) was Prepared at 180°C for 4 hours by using an unpretentious hydrothermal method. $TiO_2$ was inspected by using field emission scanning electron microscopy (FE-SEM), transmission electron microscopy (TEM), x-ray diffraction spectroscopy, and UV-visible spectroscopy. This work expresses the construction of dye-sensitized solar cells (DSSCs) from $TiO_2$ thin films with complex Ni-azo dye and azo ligand. The spectroscopic studies (Fourier-transform infrared spectroscopy (FTIR), UV-vis, and Proton Nuclear Magnetic Resonance ($^1$H-NMR)) are used to identify the azo ligand and its complex Ni (II) to synthesize the $DSSC_S$. Current-Voltage (I-V) characteristics show that the DSSCs is the highest change efficiency for $TiO_2$/ Ni-azo dye than $TiO_2$/azo dye, about 2.30% and 1.88%, respectively, under 100 mW/cm$^2$ standard visible light.

**Keywords:** Dye-sensitized, Efficiency, Ni-azo dye, Solar cells (DSSCs).

International Journal of Drug Delivery Technology (2022); DOI: 10.25258/ijddt.12.2.24

**How to cite this article:** Sahap EH, Sajad FAA, Al-Labban HMY. Incorporation of Nickel with Azo Dye and its Applications in Dye-Sensitized Solar Cells. International Journal of Drug Delivery Technology. 2022;12(2):603-609.

**Source of support:** Nil.

**Conflict of interest:** None

## INTRODUCTION

Since the 1990s, a third-generation solar cell (DSSCs) has garnered a lot of interest and been respected as a substitute for fossil fuel energy. To reduce the cost, we preferred solar cells to conventional silicon-based cells (Obaid *et al*., 2020).[1] The solar cells are characterized by flexibility in the shape, Smooth access to dye resources, and Great achievement DSSC Transformation of sunlight into electrical energy Symmetry the photocomposition operation Through the use of artificial or natural dye as light harvest tincture (Kwak *et al.* 2021).[2] Photo sensor in the solar cell absorbs photons and urges on the excitement of electrons to the broadband gap semiconductor, dyes, and electrolyte (Jabbar & Latif, 2021).[3] The Ruthenium complex is one of the most efficient light-harvesting sensitizers mentioned in DSSCs because of the great risks of these materials being sensitive to ruthenium (Huan, 2020).[4] These are complicated procedures In terms of increased cost, environmentally unsafe, and carcinogenic (Chan *et al*., 2019).[5] Thermal stability, strong absorption in the visible region, and intrinsic advantages of a good photo for organic dye such as azo benzene have prominent chromospheres. Azo benzene is a reactive essential for functional group diversion and connection such as alkoxy and vinyl chain with amended optical properties during the initial photo excitation (Yesodha *et al*., 2004).[6] The mechanism of a traditional damp type DSSC containing redox couples in the electrolyte is shown in Figure 1 by Murakoshi *et al*. (1989).[7] The photo anode, made of a nonporous dye-sensitized and n-type semiconductor, receives electrons from the photo-excited dye sensitizer, thereby oxidizing to S+. The neutral dye sensitizer (S) can be renewed by the oxidation reaction (RO) of the redox species dissolved in the electrolyte, which is usually $I_3$-/I-. The mediator R will then be renovated by reduction at the cathode (OR) by the outer circuit the electrons circulated through it (Jang *et al*. 2020).[8]

Heterocyclic azo dyes compounds and their complexes are used in the manufacture of dyes and electromagnetic materials, and in the printing process, in addition to nonlinear optical elements (Witwit *et al*., 2019).[9] Considered the imidazole azo

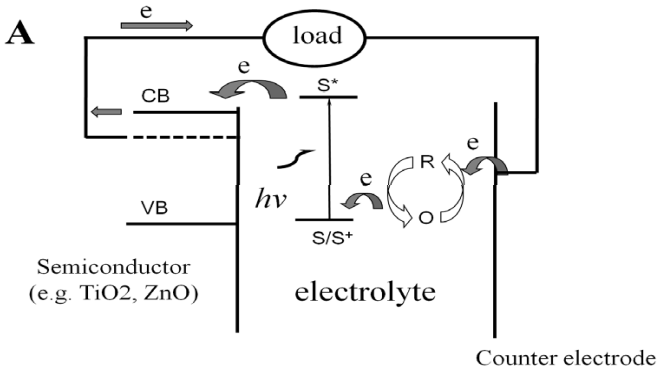


**Figure 1:** Operation mechanism of the dye-sensitized electrochemical solar cell (Murakoshi *et al*., 1989).

*Author for Correspondence: emanh.hamza@uokufa.edu.iq

and its derivatives are assigned as heterocyclic compounds, and it has lots of uses in various fields. And it is used in chemical and biological applications such as Appreciation for many metal ions (Chhetri *et al*., 2021).[10] Complexion agents, dyeing materials, antidepressants, tubercular ant agents, and models for biological systems. Hence, Metal complexes chelates of azo dyes are considered a higher important component in dyeing the wool; nylon and silks lead to higher fastness for washing and light (Pielesz *et al*. 2000).[11] In the current study, 2-[(4-acetophenone)azo]-4;5-diphenyl imidazole (4-ACPI) and its complex with Ni(II) are synthesized. The photoelectric properties of a nickel complex (II) as a sensor have been studied for the first time. The Mentioned compound's structural, morphological, and optical properties were also identified.

## MATERIALS AND METHODS

The materials for this research are from Merck company and have been used without Re-purify. The conductive glass slides are coated ITO- (Indium- tin oxide) (surface resistivity 16 Ω/sq, thickness 2.3 mm) obtained from China and were used as substrates for preparing $TiO_2$ thin films electrode and a carbon cathode electrode.

### Preparation of Ligand

*Preparation of the First Compound 5,4-diphenylimidazole*

75 mL of ice acetic acid was added to a mixture of (2.1 g, 0.01 mole) of benzyl and (0.28 g, 0.002 mole) of hexamethylene tetramine and (5.75 g, o.175 mole) of ammonium acetate., then the mixture was stepped up for 1 hour using a reflecting condenser. Then the solution was transferred to a beaker capacity (1 L) and after cooling it was diluted by adding (200 mL) of distilled water, and then the ammonium hydroxide solution was added drop by drop to neutralize the solution and obtain A white precipitate, the precipitate was filtered after the sedimentation process was completed and washed with distilled water several times to get rid of the excess base residues and salts. It was air-dried, recrystallized with ethanol, and then left to air dry (Al-Labban, 2017).

*Preparation 2-[(4 - acetophenone)azo] -4,5-diphenyle imidazole (4-ACPI)*

The Shibata method was adopted to prepare the ligand of 2-[ (4- acetophenone) azo]-4,5-diphenyl imidazole, including 4-amino acetophenone and the nitrogen pairs coupled with the imidazole derivative in an alcoholic base environment (Li *et al*., 2014). Using the mixture from (10ml distal water; 2 mL conc. HCl) to melt (0.675g; 0.005mole) from 4-amino acetophenone , Cool the mixture to (0-5) ºC and add to it (0.69 g, 0.01 mole) of sodium nitrite dissolved in (10 ml) of distilled water drop by drop with constant stirring and note that the temperature does not rise above 5ºC. The diazonium salt solution was dropped on a basic alcoholic solution of (4,5-diphenyl imidazole 1.1 g; 0.005 moles) with cooling under 5ºC; a Reddish orange color was observed; this colored solution was saved for 24 hours. Then the pH value of the solution is corrected to 7 with dilute HCl solution Deposits are observed, allowed to settle, and then dried in the air. The following diagram shows the course of the reaction to prepare the azo compound (Adam *et al*. 2019).

### Synthesis of Ni (II) complex

(0.0336 g; 0.0001 mole) of (4-ACPI) dissolved in (10 mL) of alcohol was appended slowly with stirring to the (0.0118 g; 0.00005 mol) of $NiCl_2.6H_2O$ that dissolved in (5 mL) of DW after cooling the reaction mixture, it was filtered and washed several times with DW water and allowed to settle and then dried in the air (Fu *et al*., 2020) (Figure 2).

*Preparation of the Working Electrodes*

First, $TiO_2$ is prepared by adding 8 mL of isopropanol dropwise to 2 mL of 5.27 M titanium tetrachloride with constant stirring to obtain TTIP (Titanium Tetra Iso Propoxide) $Ti(OC_3H_7)_4$. A 1.0 mL from (TTIP) is added to 5.8M of HCl. To 70 mL Teflon-lined stainless-steel autoclave, the prepared mixture is transferred and fixed inside the oven at a temperature of 180 ºC for 4 hours. The autoclave is left to cool at room temperature after completing the preparation. A white precipitate is obtained, and the product is washed with deionized water (DW) and ethanol three times using a centrifuge at 500 rpm and dried at 80ºC for 30 minutes. The product is annealed at 450 ºC for 3 hours to enhance crystallinity (Cinti *et al*., 2019).[12] The ITO glass slides are well cleaned using isopropanol for 5 minutes, followed by acetone for another 5 minutes.

Finally, all cleaned substrates are washed using DIW and dried with hot air. To apply the $TiO_2$ paste, ensure the

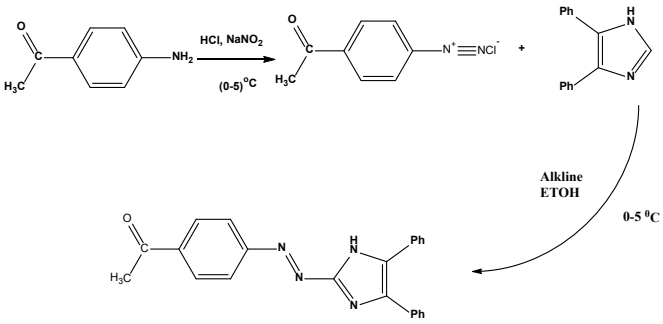


**Scheme 1:** Synthesis of azo ligand

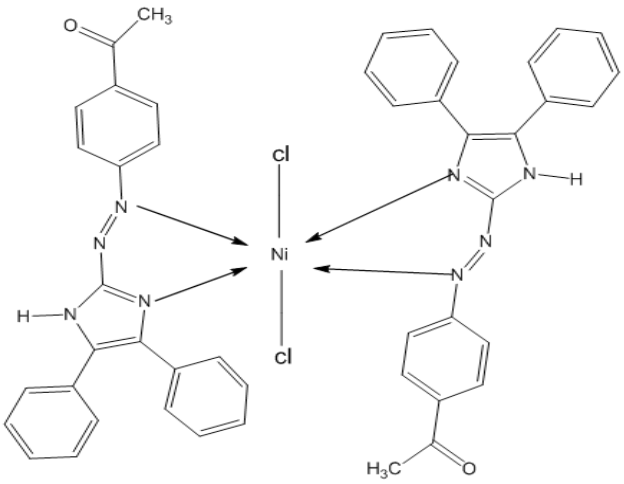


**Figure 2:** Ni complex with (4-ACPI)

conductive side of the glass is up; with the 3M scotch tape, tape down two parallel edges of the glass to a flat surface. Using a capillary pipette, apply a few drops of the $TiO_2$ paste, which is prepared by mixing 0.2 g from NPS-$TiO_2$ with a few drops of dilute acetic acid onto the glass (doctor blade process). Quickly rub a flat edge over the surface to spread the paste smoothly. Let it sit for a few minutes, and remove the tape. Cover the hot plate with aluminum foil and place the electrode, conductive side up on the plate; heat the plate to 400°c and let it sinter for about 30 minutes. You will see the white paste turn brownish. Eventually, that material will take off, and the electrode will be all white. Take the entire piece of aluminum foil off the hot plate to allow the electrode to cool off. Finally, the prepared electrode are immerged inside a 20mg/L of nickel (Ni) complex with 2-[(4 amino acetophenone) azo] -4;5-diphenyl imidazole (4-ACPI) at once and with 2-[(4 amino acetophenone)azo] -4;5-diphenyl imidazole (4-ACPI) dey solution at another once for 24 hours in the dark place to prevent dye photo degradation. The surface of NPs-$TiO_2$ films is washed with ethanol to remove non adsorbed dye molecules (Lokman *et al*., 2019).[13]

*Preparation of Counter Electrode*

A counter electrode was developed from a thin carbon layer on an ITO plate. A carbon black electrode was easily made by moving the substrate (conductive side of ITO) above the flame of a candle, as shown in Figure 3. The substrate became black after some time, and then it was cooled; a few drops of ethanol were added to the dried surface for diffusion across the carbon layer and the substrate was further dried (Aftabuzzaman *et al*., 2020).[14]

**Redox, Electrolyte, Between Two Electrodes**

Iodine/ iodide electrolyte is prepared by dissolving 10 g of potassium iodide (KI) in 25 mL of deionized water (DI) using a 100mL glass-stoppered flask. Then, a 3.175 g of iodine (I2) was added to the solution with continuous shaking until dissolving all materials (Iftikhar *et al*., 2019).[15]

**Figure 3:** Prepared carbon-coated counter electrode by using candle fumes.

**Device Fabrication of DSSC**

The solar cell consists of seven layers arranged by placing a double-sided adhesive tape over the outer area of the adsorbed dye on the ITO glass with TiO2 film surface. The photoanode and cathode were fabricated into a sandwich-type cell. Iodine/ iodide electrolyte solution was injected into the cell to ensure that the electrolyte did not spill outside the mask.

## RESULTS AND DISCUSSION

**The $^1$HNMR Spectrum of the Ligand**

$^1$H-NMR spectrum δ(ppm) (Figure 4) of compounds [A] showed the following characteristic signals (DMSO-$d_6$ as a solvent): δ(C-H) Aromatic rings at δ(7.26-8.18)ppm that could be attributed to the aromatic protons for three phenyl rings, δ (s-CO–CH3) at δ (2.65) ppm and δ (–NH imidazole rings) at δ (13.65) ppm[9]

**IR Spectra**

The wave numbers of some characteristic bands in the IR spectra of ligand, The stretching vibration of (N-H) groups at (3419 $cm^{-1}$) back to the imidazole $^{ring.}$ When compared with the metal complex band, no significant change was observed (The ν(N═N) stretching vibration appears at (1440 cm-1) of the imidazole ring, which was showed a medium band at 1448 $cm^{-1}$ when complexion. This group has observed changes in the size and strength of the metal complexes spectra, which proves their involvement in the coordination process (Kataoka *et al*., 2020).[16] Appear the spectrum of the prepared complex a new weak band at the frequency (420 $cm^{-1}$) due to the metal bonding to the nitrogen atom (M-N), and The ligand spectrum is free of this band. The Table 1 shows the information mentioned about the ligand and its complexity.

**UV-Visible spectroscopy**

Electronic spectra of the ligand showed three major absorption bands in alcohol within the range of 200–800 nm. The first at 442 nm is related to n-π* transitions, and bands at 210 nm are due to π–π* transitions for imidazole molecule, while the third band is due to ( π- π*) transition for benzene ring Paired with imidazole ring throw (N=N) group. When comparing the color

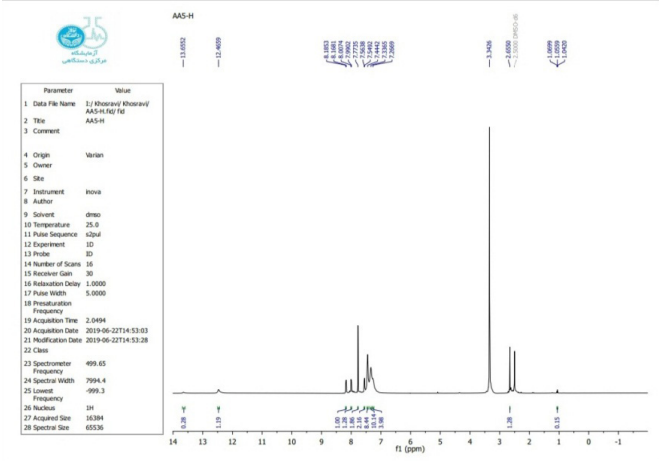


**Figure 4:** $^1$H-NMR Spectrum of Compound [A]

and absorption positions between ligand and its complexes, we observed a clear difference in color and shifting in absorption position (λmax) toward higher wavelength[s] (Nienhaus & Nienhaus, 2005).[17] This may be referred to coordination and complex formation between ligands and these ions as shown in Figures 7 and 8.

The important parameter to determine the DSSC efficiency is the optical properties of the dye adsorption on the TiO2 surface. The dye molecules collected light and produced excitation of electrons (Hossain *et al*., 2018);[18] therefore, the Ni complex ($NiL_2Cl_2$) dye has been higher λmax than ligand ($C_{23}H_{18}N_4O$) that were carried out Ni complex the best efficiency of DSSC.

## X-Ray Diffraction

The x-ray diffraction pattern of the synthesized tetragonal anatase $TiO_2$ nanoparticles agrees with the JCPDS card no.

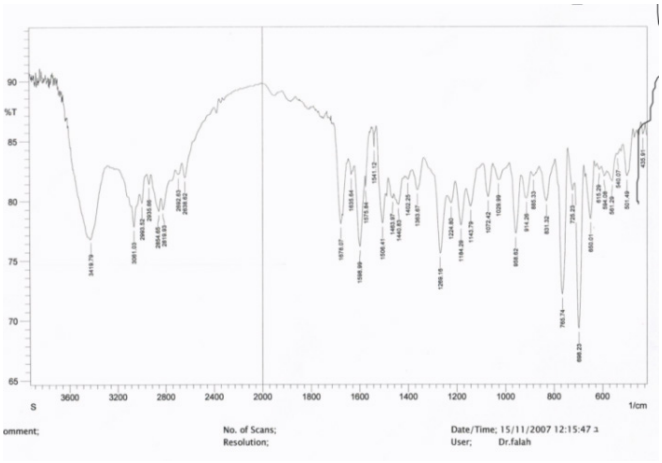


**Figure 5:** The FT-IR spectrum of the (4-ACPI).

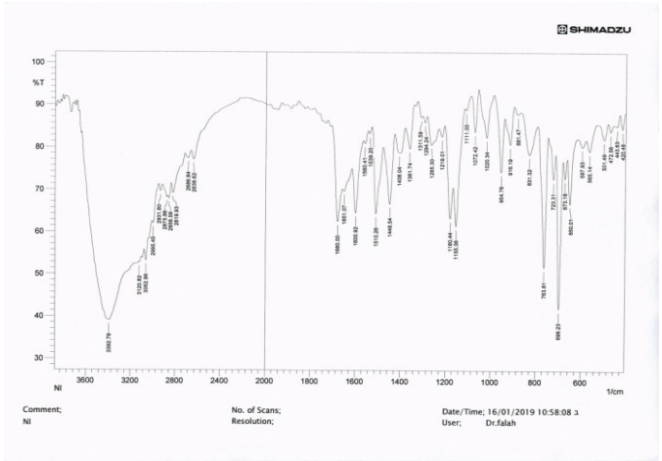


**Figure 6:** FTIR spectrum of the Ni(II) complex

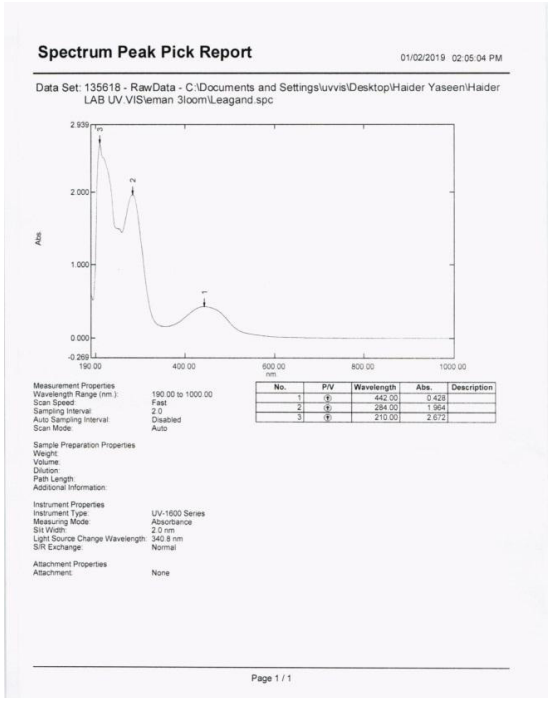


**Figure 7:** UV-Visible spectra for the Ni complex

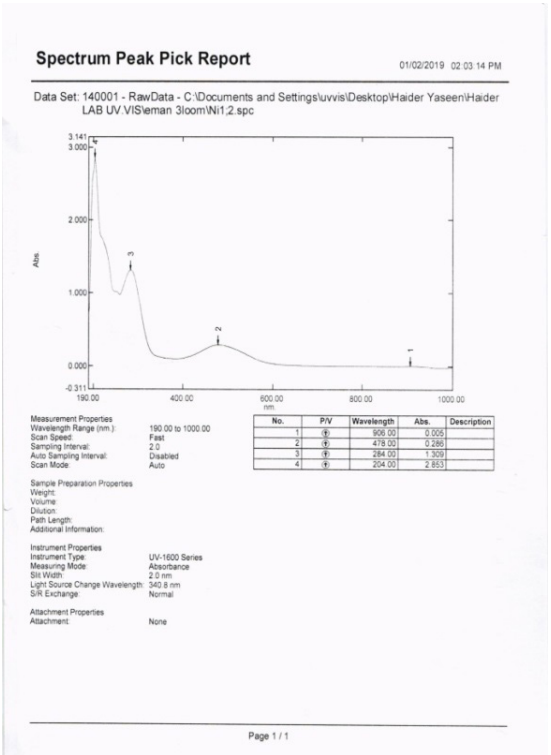


**Figure 8:** UV-Visible spectra for the ligand

**Table 1:** IR vibrations of ligands and their complex

| *M-N* | *v(N=N )* | *v (C=N) imidazole* | *v(C=O)* | *v( C-H)Ar. v( C-H)aliph* | *v( N-H)* | *Compound* |
|---|---|---|---|---|---|---|
| – | 1440w | 1598s | 1678s | 3061m<br>2993w | 3419s | $C_{23}H_{18}N_4O$ |
| 420 | 1448m | 1600s | 1680s | 3062m<br>2995m | 3992s | $[NiL_2Cl_2]$ |

**Table 2:** Photo electrochemical parameters of the DSSCs, A = 1.5cm$^2$, under intensity light 100 m W/cm$^2$

| Anode electrode | Isc(mA) | Voc(V) | Imax(mA) | Pmax(mW/cm$^2$) | FF% | η% |
|---|---|---|---|---|---|---|
| $TiO_2$ / Ni-Azo dye | 8.00 | 0.69 | 7.60 | 3.38 | 61.2 | 2.30 |
| $TiO_2$/Azo dye | 7.15 | 0.65 | 6.70 | 2.81 | 25.6 | 1.88 |

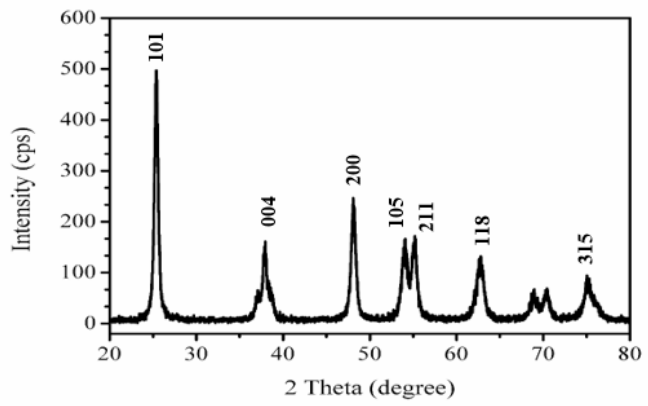


**Figure 9:** X-ray diffraction pattern of NC-$TiO_2$.

21-1272 is shown in Figure 9. The 2θ peaks at 25.27° and 47.01° endorse its anatase structure (Bui *et al*., 2019).[19] The X-ray intensity of the sample indicates that the shaped nanoparticles are crystalline, and expansion diffraction peaks refer to small crystallite. The absence of false differ- action refers to the purity of the sample.

### The Field Emission Scanning Electron Microscope (FESEM) and Transmission Electron

*Microscopy (TEM) Analysis*

The FESEM image of $TiO_2$ nanoparticles prepared using the hydrothermal method (Kumar *et al*., 2019) is shown in figure 10. The particle size is ranged from 25 nm to 35 nm with a spherical shape. The TEM gives the particles shapes of NC-$TiO_2$ seem as nano plates with very thin Nanochips and a size ranging from 15 to 60 nm, as shown in Figure 11.

### The I-V Characteristics of DSSC.

I-V characteristics of DSSC showed in Figure 12. The following equations determined the general efficiency (η) (Buene *et al*. 2019).[20]

$$FF = V_m J_m / V_{oc} J_{sc} \quad (3)$$

$$\%\eta = [V_{oc} J_{sc} FF / P_{in}* A] \times 100 \quad (4)$$

Where $P_{in}$ is the power incident light on the solar cell, $J_{sc}$ is short-circuited current density at zero voltage, $V_{oc}$ is the open-circuit voltage at zero current density, $J_m$ is the maximum current density, $V_m$ is maximums voltage, and FF is the fill factor. All the results are abridged in Table 2. It is clearly shown that the DSSC efficiency of NC-$TiO_2$ with Ni complex azo dye is greater than the DSSC efficiency of NC-$TiO_2$ with azo dye.

The DSSCs is fabricated using $TiO_2$ nanoparticles as a photoanode electrode with Ni complex ($NiL_2Cl_2$) dye and azo dye ($C_{23}H_{18}N_4O$) as absorber media. Figure 12 shows the I-V characteristics of DSSCs prepared based on $TiO_2$/Ni azo dye and $TiO_2$/azo dye. However, $TiO_2$/ Ni azo dye has shown $V_{OC}$ of 0.69V and $I_{SC}$ of 8.0mA to give conversion efficiency

**Table 3:** The values of the greatest wavelength of the solutions of the ligand and its prepared complex

| Complex | Max λ | Color |
|---|---|---|
| $C_{23}H_{18}N_4O$ | 442 | Reddish orange |
| $[NiL_2Cl_2]$ | 478 | Reddish-brown |

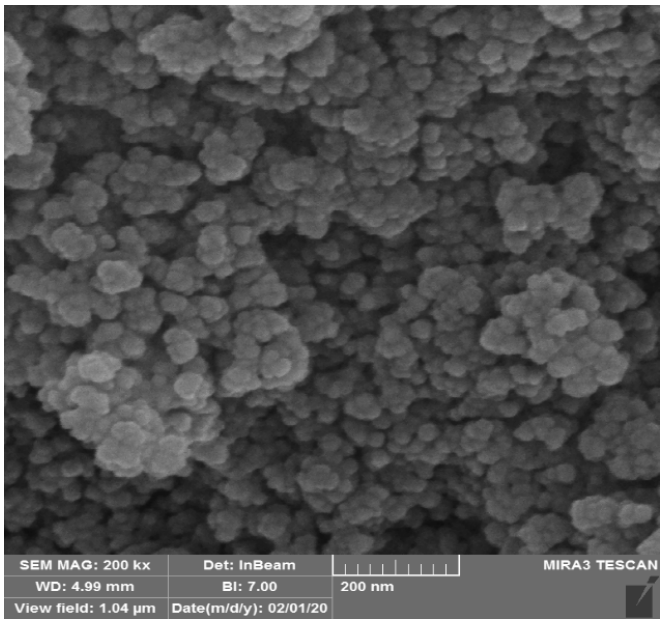


**Figure 10:** FE-SEM image of $TiO_2$

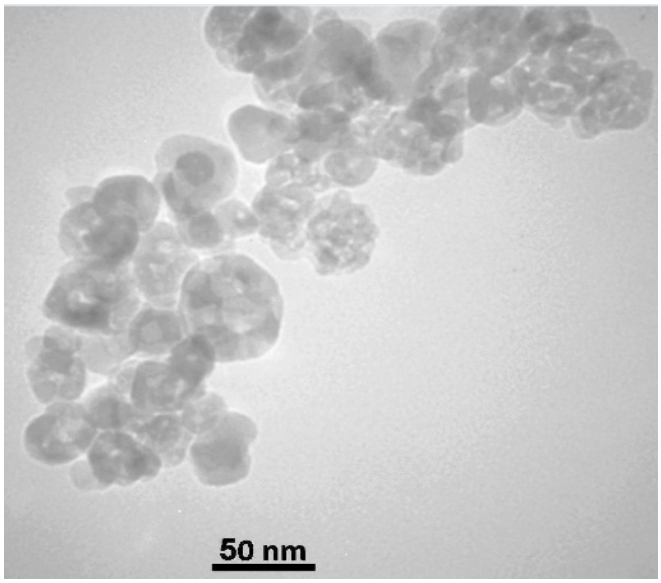


**Figure 11:** TEM image of $TiO_2$ nanoparticles

(η) of 2.30%, while $TiO_2$/azo dye DSSCs have shown $V_{OC}$ of 0.65V and $I_{SC}$ of 7.15mA to give η of 1.88% (Table 3). The results reveal that the efficiency of DSSC is fabricated based on NC-$TiO_2$ with Ni azo dye is higher than those fabricated

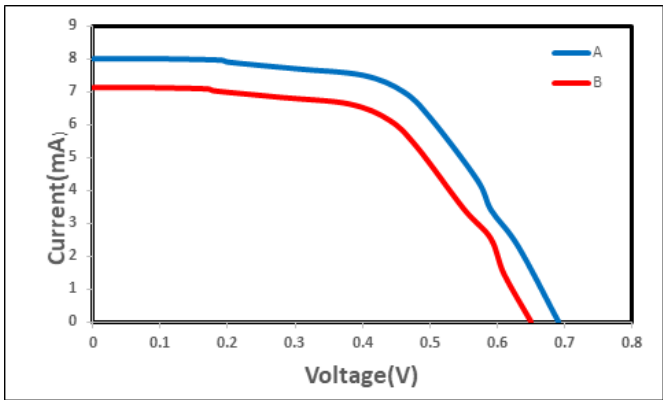


**Figure 12:** Compered to I-V measurement for the two dyes sensitized solar cells: (A) $TiO_2$ / Ni-Azo dye Voc = 0.690v, Jsc = 5.333mA/cm$^2$, FF = 0.612, $\eta$% =2.30 (B) $TiO_2$ / Azo dye Voc = 0.650V, Jsc = 4.766mA/cm$^2$, FF = 0.256,$\eta$% = 1.88%

based on $TiO_2$/azo dye. The reason, perhaps the Ni complex ($NiL_2Cl_2$) dye has been higher λmax than ligand ($C_{23}H_{18}N_4O$) (Supriyanto *et al*. 2019: Al-Labban *et al*. 2019).[21,22] This means that the energy gap between the highest-occupied molecular orbital (HOMO) and lowest unoccupied molecular orbital (LUMO) decreases were carried out Ni complex the best efficiency of DSSC. The fabricated DSSCs are also due to the intensity (100 mW/cm$^2$) of the light source used (AL-labban & ALjanaby 2020).[23]

## CONCLUSION

The complex of $NiL_2Cl_2$ and $C_{23}H_{18}N_4O$ azo dye was synthesized at ( 0 – 5) C$^o$. The photovoltaic properties of $NiL_2Cl_2$ and $C_{23}H_{18}N_4O$ azo dyes used as sensitizer dyes was studied for the first time. The conversion power efficiency of $NiL_2Cl_2$ and $C_{23}H_{18}N_4O$ azo dyes-based solar cell was calculated as 2.30% and 1.88%, respectively. Using photovoltaic parameter determined from I-V curve, the synthesized $NiL_2Cl_2$ and $C_{23}H_{18}N_4O$ azo dye was investigated in terms of structural, morphological, and optical properties, respectively. Consequently, $NiL_2Cl_2$ and $C_{23}H_{18}N_4O$ azo dyes can be used as a suitable sensitizer in the application of DSSCs.

## REFERENCE


1. Obaid NH, Kadhim AA, Khazaal MH. Preparation, Synthesis New Azo Ligand (E)-1-(3-((E)-(4, 5-diphenyl-1H-imidazole-2-yl) diazenyl) phenyl) ethanone Oxime and Some of its Metal Complexes. NeuroQuantology 2020;18(9):96.
2. Kwak JI, Kim L, Lee TY, Panthi G, Jeong SW, Han SH, Chae H, An YJ. Comparative toxicity of potential leachates from perovskite and silicon solar cells in aquatic ecosystems. Aquatic Toxicology 2021; 105900.
3. Jabbar FH, Latif WA. A Comparative Analysis of Various Types of Modified Bentonite Clays Added to Poly Methyl Butadiene for Nanocomposite Preparation. NeuroQuantology 2021; 19(1):67-71.
4. Huan H, Jile H, Tang Y, Li X, Yi Z, Gao X, Chen X, Chen J, Wu P. Fabrication of ZnO@ Ag@ Ag3PO4 ternary heterojunction: superhydrophilic properties, antireflection and photocatalytic properties. Micromachines 2020; 11(3):309.
5. Chan KM, Vasilev K, Shirazi HS, McNicholas K, Li J, Gleadle J, MacGregor M. Biosensor device for the photo-specific detection of immuno-captured bladder cancer cells using hexaminolevulinate: An ex-vivo study. Photodiagnosis and photodynamic therapy 2019 ;28:238-47.
6. Yesod SK, Pillai CK, Tsutsumi N. Stable polymeric materials for nonlinear optics: a review based on azobenzene systems. Progress in Polymer Science 2004; 29(1):45-74.
7. Murakoshi K, Kogure R, Wada Y, Yanagida S. Fabrication of solid-state dye-sensitized TiO2 solar cells combined with polypyrrole. Solar Energy Materials and solar cells 1998; 55(1-2):113-25.
8. Jang YJ, Thuy CT, Thogiti S, Cheruku R, Ahn KS, Kim JH. Electrochemically Deposited Polypyrrole for Counter Electrode of Quasi-Solid-State Dye-Sensitized Solar Cell. Journal of nanoscience and nanotechnology 2020; 20(1):546-51.
9. Witwit IN, Mubark HM, Al-Labban HMY. Synthesis and characterization of new imidazole azo ligand with some of transition metal ions, and their biological effect on two pathogenic bacteria of burn patients. International journal of research in pharmaceutical sciences 2019; 10(3):1847–1856.
10. Chhetri A, Chettri S, Rai P, Mishra DK, Sinha B, Brahman D. Synthesis, characterization and computational study on potential inhibitory action of novel azo imidazole derivatives against COVID-19 main protease (Mopar: 6LU7). Journal of molecular structure 2021; 1225:129230.
11. Pielesz A, Włochowicz A, Biniaś W. The evaluation of structural changes in wool fibre keratin-treated with azo dyes by Fourier Transform Infrared Spectroscopy. Spectrochimica Acta Part A: Molecular and Biomolecular Spectroscopy 2000; 56(7):1409-20.
12. Cinti S, Moscone D, Arduini F. Preparation of paper-based devices for reagentless electrochemical (bio) sensor strips. Nature protocols 2019;14(8):2437-51.
13. Lokman MQ, Shafie S, Shaban S, Ahmad F, Jaafar H, Mohd Rosnan R, Yahaya H, Abdullah SS. Enhancing photocurrent performance based on photoanode thickness and surface plasmon resonance using Ag-TiO2 Nanocomposites in dye-sensitized solar cells. Materials 2019; 12(13):2111.
14. Aftabuzzaman M, Kim CK, Zhou H, Kim HK. In situ preparation of Ru–N-doped template-free mesoporous carbons as a transparent counter electrode for bifacial dye-sensitized solar cells. Nanoscale 2020;12(3):1602-16.
15. Iftikhar H, Sonai GG, Hashmi SG, Nogueira AF, Lund PD. Progress on electrolytes development in dye-sensitized solar cells. Materials 2019; 12(12):1998.
16. Kataoka K, Ito T, Okuda Y, Sakai Y, Yamashita S, Sakurai T. Roles of the indole ring of Trp396 covalently bound with the imidazole ring of His398 coordinated to type I copper in bilirubin oxidase. Biochemical and biophysical research communications 2020; 521(3):620-4.
17. Nienhaus K & Nienhaus GU. Probing heme protein-ligand interactions by UV/visible absorption spectroscopy. In *Protein-Ligand Interactions* 2005; (pp. 215-241). Humana Press.
18. Hossain MK, Pervez MF, Uddin MJ, Tayyaba S, Mia MN, Bashar MS, Jewel MK, Haque MA, Hakim MA, Khan MA. Influence of natural dye adsorption on the structural, morphological and optical properties of TiO2 based photoanode of dye-sensitized solar cell. Mater Sci.-Pol. 2018; 36:93-101.
19. Bui VK, Park D, Pham TN, An Y, Choi JS, Lee HU, Kwon OH, Moon JY, Kim KT, Lee YC. Synthesis of MgAC-Fe 3 O 4/TiO 2

hybrid nanocomposites via sol-gel chemistry for water treatment by photo-Fenton and photocatalytic reactions. Scientific reports 2019 ;9(1):1-1.

20. Buene AF, Christensen M, Hoff BH. Effect of Auxiliary Donors on 3, 8-Phenothiazine Dyes for Dye-Sensitized Solar Cells. Molecules 2019; 24(24):4485.
21. Supriyanto E, Kartikasari HA, Alviati N, Wiranto G. Simulation of dye-sensitized solar cells (DSSC) performance for various local natural dye photosensitizers. IOP Conference Series: Materials Science and Engineering 2019; 515(1): 012048. IOP Publishing.
22. Al-Labban HMY. Synthesis, characterization, and study of biological activity of some new 1, 2, 3, 4-Tetrazole derivatives. Research Journal of Pharmacy and Technology 2017;10(10):3645-52.
23. AL-labban HMY & ALjanaby AAL. An overview of some heterocyclic organic compounds; synthesis, characterization, thermal properties and antibacterial activity. International Journal of Pharmaceutical Research 2020; Supplementary Issue 1 :2394-2399.